Adsorption of phenol on graphite(0001) and α-Al_2O_3(0001): Nature of van der Waals bonds from first-principles calculations

Svetla D. Chakarova-Käck,[1] Øyvind Borck,[1,2] Elsebeth Schröder,[1] and Bengt I. Lundqvist[1]
[1]*Department of Applied Physics, Chalmers University of Technology, SE–412 96 Göteborg, Sweden*
[2]*Department of Physics, Norwegian University of Science and Technology, NO–7034 Trondheim, Norway*
(Received 3 June 2006; published 3 October 2006)

First-principles calculations of phenol adsorbed on two different surfaces, graphite(0001) and α-Al_2O_3(0001), are performed with traditional semilocal density functional theory (DFT) and with a recently presented density functional (vdW-DF) that incorporates the dispersive van der Waals (vdW) interactions [Phys. Rev. Lett. **92**, 246401 (2004)]. The vdW-DF is of decisive importance for describing the vdW bond of the phenol-graphite system and gives a secondary but not negligible vdW contribution for phenol on alumina. We find a predominantly covalent bond at the alumina surface. There, adsorption results in a binding separation (distance between surface Al and the O of the inclining phenol molecule) of 1.95 Å and a binding energy of 1.00 eV, evaluated within the generalized gradient approximation (GGA) of DFT, i.e., from covalency, with the energy increasing to around 1.2 eV when the contribution from vdW interactions is also accounted for. On graphite, with its pure vdW bond, the adsorption distance (separation between parallel surface and phenol molecule) is found to be 3.47 Å and the adsorption strength 0.56 eV. Comparison of the results for alumina and graphite mutually and with published results for nickel reveals significant differences in the adsorption of this model biomolecule.

DOI: 10.1103/PhysRevB.74.155402 PACS number(s): 68.43.Bc, 34.30.+h, 71.15.Mb, 31.15.Ew

I. INTRODUCTION

Phenol (C_6H_5OH), a small but important organic molecule, consists of a benzene ring, where one hydrogen atom is substituted by an OH group. In the amino acid *tyrosine* phenol is a side group, making phenol relevant for protein folding and protein adsorption.[1] Phenol also appears as end or side group in a number of polymers and therefore likewise plays an active role in the polymer adhesion processes, for instance, for paint adhesion on surfaces. Adsorption of phenol on Si is interesting for the development of new semiconductor materials.[2] Further, phenol is a frequent and toxic byproduct in industrial processes and is thus interesting from an environmental perspective. Physisorption due to dispersive forces is the mechanism behind the use of activated carbons for removing phenol from aqueous solutions, important from industrial and environmental perspectives.[3]

Atomic-scale studies of phenol adsorption are rare, in particular modern first-principles theory studies on different kinds of substrates. Earlier studies include mainly phenol adsorption on nickel in connection with polymer adhesion studies.[4] We here present first-principles density functional theory (DFT) calculations of phenol adsorption on graphite and alumina [α-Al_2O_3(0001)], representatives both of important classes of materials (dielectric and ionic) and surfaces (hydrophobic and hydrophilic). They are anticipated to have different adsorption mechanisms with significantly different strengths, as confirmed by our calculated results, adsorption energies found being roughly 0.56 and 1.2 eV on graphite and alumina, respectively, as compared to the value 0.9 eV found in the recent study of phenol on the metallic Ni(111) surface.[4] Behind these three numbers there are three quite different adsorption mechanisms whose natures are revealed below by in-depth studies of the adsorbate-induced electronic structures.

For calculations of electronic structure, bonding, structure, and elasticity, DFT has proved to be a powerful tool. However, the traditional implementations lack the ability to describe dispersive interactions, which are important for, e.g., vdW complexes and the phenol-graphite binding. Hence, the standard DFT in the generalized gradient approximation (GGA) is here supplemented by a van der Waals density functional (vdW-DF) that incorporates the dispersive vdW interactions into DFT.[5]

Phenol adsorption on graphite has earlier been studied by Monte Carlo computer simulations.[6] Interactions between adsorbate and adsorbent and mutually between adsorbates are there described by parameter-dependent effective potentials, aimed at accounting for dispersive and electrostatic forces.[6] Thus a configuration with the molecule lying flat a distance 3.44 Å from the surface and with a binding energy of around 0.5 eV is found. The three phenol orientations considered in Ref. 6 differ in adsorption-energy values by less than the error caused by the use of empirical atomic effective parameters, as estimated by us. In our study we find values for the adsorption energy and the binding distance similar to those in Ref. 6, however, by using a first-principles method, with only the atomic numbers as input.

The application of the vdW-DF method to the phenol system is very much encouraged by the recently found excellent agreement between theory and experiment for benzene on graphite[7] (calculated adsorption energy being 0.5 eV). This is reassuring because phenol has an electronic structure similar to that of the benzene molecule. Successful applications of vdW-DF to interaction energies of monosubstituted dimers, including phenol,[8] are also encouraging in this respect.

The rest of the paper is organized as follows: First (Sec. II) we describe the details of the density functional calculations for the graphite and alumina adsorption studies. The

description of how we include the vdW interaction is deferred to a later section. Then comes a short description of the phenol molecule in the gas phase in Sec. III. Sections IV and V focus on adsorption on graphite and on alumina, the former including a short description of the actual implementation of the vdW-DF. Finally, Sec. VI provides a discussion of our results.

II. METHOD

All calculations presented here are based on the plane-wave implementation DACAPO[9] of DFT. To account for exchange and correlation, three different functionals are used: (a) the standard GGA in the PW91 flavor,[9,10] (b) the GGA in the revPBE flavor,[9,11] and (c) the vdW-DF.[5] GGA has well proved its abilities to describe short-range interactions in strongly bonded systems. Where vdW forces usually can be ignored (such as the isolated gas-phase phenol molecule, the alumina surface, and within a sheet of graphene) GGA is used for determining the atomic structure and energy of each isolated object, the differences between PW91 and revPBE here being negligible. For phenol adsorption on graphite, however, the GGA's need to be extended by explicit inclusion of the vdW interactions, here done in vdW-DF.[5] The ubiquitous vdW forces contribute also to the adsorption of phenol on alumina, and we perform vdW-DF calculations on this system to assess the magnitude of the contribution, in particular in relation to other contributions.

The structure, lattice parameters, and energetics for the clean graphite and alumina surfaces have previously been determined with the same or similar codes and choices of pseudopotentials, yielding results consistent with other modern theoretical and experimental results.[12–15]

The graphite surface is modeled by one sheet of graphene. When calculating the interaction of phenol with graphite, we should add also the interaction energy of the second and lower sheets, below the top layer. However, already the change in the interaction when including the second layer is found small ($\approx 4\%$), so these extra contributions will be ignored here. In order to accommodate the long-range vdW interactions in a post-processing of the nonlocal-correlation energy,[5] we use a rather long (in the direction perpendicular to the sheet) unit cell of size 26 Å for the graphite adsorption system. The unit cell used in the calculations of phenol on graphene is hexagonal with a (5×5) surface unit cell, corresponding to a cell side length of 12.32 Å, which is also the nearest-neighbor separation for the adsorbed phenol molecule with its periodic images. To describe the Brillouin zone in the (5×5) surface cell we use a $2\times2\times1$ mesh of Monkhorst-Pack[16] special k-points, and the plane wave cutoff energy 450 eV.

Alumina is here represented by the Al-terminated α-$Al_2O_3(0001)$ surface. α-alumina is the stable phase, and α-$Al_2O_3(0001)$ the most stable surface, so most other alumina surfaces are more reactive. The bulk unit cell is rhombohedral with lattice parameters $a_0=5.173$ Å and $\theta=55.28°$ and with internal Wyckoff positions[17] of Al, respectively, O within the unit cell $w=0.3523$ and $u=0.5561$.

For the alumina surface we use a periodic unit cell consisting of (2×2) hexagonal surface unit cells, with one phenol molecule adsorbed per (2×2) surface unit cell, thus corresponding to a coverage of a quarter of a monolayer. This leads to a nearest-neighbor separation of 9.60 Å for the adsorbed molecule with its periodic images. The slab that models the surface consists of four layers of Al-O_3-Al, with the atomic positions of the bottom O_3 and Al layers kept fixed in the bulk structure and the remaining layers relaxed using the PW91 flavor of GGA and the Broyden-Fletcher-Goldfarb-Shanno (BFGS) algorithm.[18] We use 15 Å of vacuum between the periodically repeated images of the slab. For the alumina calculations of the (2×2) surface cell we use, as for graphite, a $2\times2\times1$ mesh of Monkhorst-Pack special k-points and the plane wave cutoff energy 450 eV. Other computational details are similar to our previous methanol-on-alumina study and are described in Ref. 14.

III. GAS PHASE PHENOL

According to our GGA calculations, the isolated phenol molecule (in the "gas phase") is flat, with values for the intramolecular bond lengths given in Table I. This is consistent with earlier experimental and theoretical reports, although some experiments[20] report a small deviation ($2°-3°$) of the OH-bond direction from the plane of the carbon ring.

The two GGA versions revPBE and PW91 give rather similar geometrical structures after BFGS relaxation, as shown in Table I. All C-C bond lengths in phenol are slightly smaller than those of graphene (1.4226 Å, when calculated in revPBE), and similar to those of benzene.

IV. PHENOL ON GRAPHITE

Phenol adsorption on graphite is calculated as that of an inert phenol molecule on a single graphene layer. The molecule is placed parallel to the surface, so that the center of its aromatic ring lies above a carbon atom in the graphite sheet (resembling the AB stacking found in graphite). This choice is analogous to what applies to benzene dimers and the related polycyclic aromatic hydrocarbon (PAH) dimers, where the slipped-parallel, i.e., AB, stacking is energetically favored.[12] The assumption that the molecules experience negligible changes in the intramolecular structure upon adsorption, relative to the gas phase structure, is based on the weakness of the dispersive adsorbate-substrate interaction compared to the intramolecular bonds, and was shown to be true for benzene dimers in Ref. 21. The potential-energy or binding curve is found by varying the separation d_{ads} between the graphene sheet and the phenol molecule with phenol kept as a rigid molecule. The phenol bond to a graphene layer positioned as the second layer of graphite is also calculated and found small (adding 4% to the binding energy), and that to further graphite layers is estimated to be negligible.

As shown in Fig. 1, there are two different AB-stacked positions for phenol: AB1 [Fig. 1(v)], when the OH group is oriented toward a carbon atom in the graphene sheet; and AB2 [Fig. 1(vi)], when it is oriented toward the center of a

TABLE I. Geometric structure of phenol (C_6H_5OH), expressed in bond lengths and C-O-H angle. The bond length $d_{CC}^{nearest}$ (d_{CC}^{far}) is the average values of the two (four) C-C bonds nearest to (away from) the OH group, and d_{CC} averages all six C-C bonds. For comparison, we also include the gas phase benzene bond lengths, calculated using the same settings as in the present (revPBE) phenol gas phase study. The bond lengths for phenol adsorbed on alumina are listed below for four different adsorption structures, while for phenol on graphite we assume that the gas-phase bond lengths are retained upon adsorption, as discussed in the text.

	$d_{CC}^{nearest}$ (Å)	d_{CC}^{far} (Å)	d_{CC} (Å)	d_{CH} (Å)	d_{CO} (Å)	d_{OH} (Å)	∠COH (°)
Gas phase phenol							
This study, revPBE	1.399	1.395	1.396	1.091	1.374	0.980	109.3
This study, PW91	1.397	1.393	1.394	1.091	1.372	0.980	109.3
Gaussian, AM1 Ref. 6	1.404	1.394	1.397	1.099	1.377	0.968	107.9
B3LYP/6-311+G(3*df*,2*p*), Ref. 19	1.3926	1.3898	1.3907	1.0822	1.3664	0.9618	109.895
CCD/6-31G*, Ref. 19	1.3959	1.3949	1.3952	1.0886	1.3746	0.9705	108.760
Expt., Ref. 20	1.3912	1.3944	1.3933	1.0828	1.3745	0.9574	108.7
Phenol on alumina							
This study, "tilted" (ii) PW91	1.387	1.393	1.392	1.091	1.405	0.988	112.9
This study, (i) PW91	1.386	1.398	1.392	1.090	1.424	0.986	109.4
This study, (iii) PW91	1.387	1.390	1.391	1.090	1.409	0.987	110.0
This study, (iv) PW91	1.386	1.390	1.392	1.090	1.416	0.989	110.9
Gas phase benzene							
This study, revPBE			1.396	1.091			

ring in the sheet. We find almost identical results for the two structures (Table II).

As shown in Table II, the GGA's (PW91 and revPBE) produce very little binding for phenol on graphite. From earlier studies[7] we know that this is the case also for benzene on graphite, where the small binding predicted by PW91 is in large contrast to the experimental data. Similar problems with standard GGA implementations arise whenever the vdW dispersive forces dominate the actual bond, as inherent to graphitic systems. These problems have long been known.[15,22] Any apparent attraction in GGA at these separations is a result of inadequate representation of exchange [21] and correlation in the tails of the electron distribution. In order to provide a proper description of the system, we here benefit from the virtues of the vdW-DF density functional[5] with vdW interactions in addition to the traditional GGA-DFT. In the vdW-DF, the nonlocal correlation part of the energy is included by calculating the total energy in the following manner:

$$E_{\text{vdW-DF}} = E_{\text{GGA}} - E_{\text{GGA},c} + E_{\text{LDA},c} + E_c^{\text{nl}}, \qquad (1)$$

where the correlation $E_{\text{GGA},c}$ is substituted by a local one, $E_{\text{LDA},c}$, and a nonlocal correlation part E_c^{nl}. The latter contains the correlation effects with a nonlocal dependence on the density and is approximated in the fashion described in Ref. 5, i.e., via the general-geometry density functional. For reasons described in more detail elsewhere,[5,23] we use the exchange of the revPBE flavor, and not that of PW91, as revPBE is the GGA exchange closest to exact exchange calculations at these separations.

The nonlocal correlation E_c^{nl} used in Eq. (1) takes the form of a six-dimensional integral over the densities and a kernel and is calculated for the phenol molecule interacting with a large piece of the graphene sheet extending over a range of radius 14 Å (see Ref. 7 for details). Thus, the binding energy calculated here for phenol on graphite is calculated in the same fashion as done for benzene and naphthalene on graphite in Ref. 7. There, a direct comparison to experimental data is made—thermal desorption measurements give an adsorption-energy value for benzene on graphite of 500 meV,[24] which is very well reproduced by the vdW-DF result (495 meV). The same vdW-DF has also been used to treat phenol dimers successfully.[8]

With vdW-DF we find the binding-energy, E_{ads}, and equilibrium-separation, d_{ads}, values shown in Table II. These are the energies for adsorption on a graphene sheet; by evaluating also the binding from the second layer of graphene in a graphite surface, namely the interaction at d_{ads} plus the layer separation in graphite, we find the energy of adsorption on a graphite surface to be approximately 4% larger than the E_{ads} given in Table II.

The earlier study of phenol on graphene by means of Monte Carlo simulations and empirical potentials using atomic effective interaction parameters[6] gave an optimum configuration with a molecule lying flat a distance 3.44 Å from the surface and with binding energy of around 6000 K (0.5 eV). The configurations treated there are of three types: (a) the center of phenol lies above a center of a graphene aromatic ring, (b) the center of phenol lies above a saddle point between two graphene carbon atoms, and (c) the center of phenol lies above a graphene carbon atom. While the third case corresponds to our two structures, Ref. 6 finds the second one to be energetically most favorable. However, the difference between the adsorption energies of the worst and the best configuration in Ref. 6 is negligible (less than 4 meV).

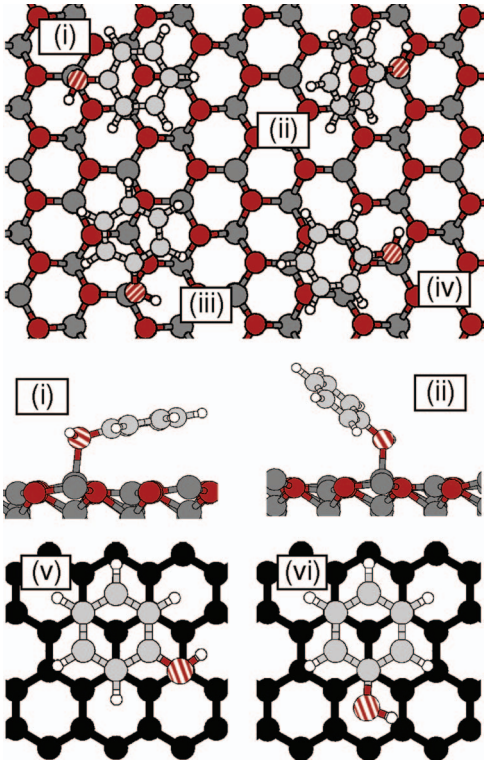

FIG. 1. (Color) Top and middle panels: Phenol on the Al-terminated α-Al_2O_3(0001) surface, showing only exposed surface atoms. The structures (i) and (ii) are also shown in a side view in the middle panels. The color coding is dark gray for aluminum atoms, alumina oxygen atoms are red, the carbon atoms of phenol are light gray, and hydrogen atoms are white. Oxygen atoms of phenol are striped, to distinguish them from the surface O atoms. Bottom panels: Phenol on a graphene sheet, in AB stacking. The carbon atoms of graphite are colored black to distinguish them from the phenol carbon atoms (light gray). The two structures in the bottom panels differ in the orientation of the OH group relative to the carbon atoms of the underlying graphene sheet. The molecule is assumed to remain flat after adsorption.

V. PHENOL ON ALUMINA

The Al-terminated α-Al_2O_3(0001) surface has the layered structure Al-O_3-Al-Al-O_3-Al-… . The unit cell exposes one layer of O atoms and three layers of Al atoms, of which one is the Al termination, as shown in the top panel of Fig. 1. We first report on the adsorption of phenol on alumina as calculated within the semilocal GGA formalism and then proceed with a description of the vdW-DF calculations.

Adsorption of phenol raises several geometric issues. For a molecule oriented with its plane flat on the surface, symmetry considerations lead to approximately 30 different possible positions and directions of phenol on the surface, counting structures with the phenol ring on top of a surface ring [like structure (iv) in Fig. 1] and structures with the phenol ring on top of one of the exposed surface atoms [like structures (i) and (iii)]. However, our previous study of methanol adsorption on the Al-terminated α-Al_2O_3(0001) surface[13,14] indicates that it is reasonable to assume that the O atom of phenol is not positioned on top of the lower-lying Al atoms or the alumina O atom, but rather adsorbs close to the top Al atom. Further, if the direction of the OH-group H atom is ignored, three relevant possible adsorption structures (approximately) parallel to the surface emerge, shown as (i), (iii), and (iv) in Fig. 1. For nonparallel (tilted) orientations, only one adsorption structure, (ii) in Fig. 1, is relevant, given that the barriers for rotation around the phenol-O-surface-Al bond are low and possible to overcome in structural BFGS relaxations.

TABLE II. Adsorption energies and separations for phenol on graphite (a single graphene sheet) and α-Al_2O_3(0001). Results of different methods are shown. The naming of the structures is given in the caption of Fig. 1.

	d_{ads} (Å)	Tilt angle (°)	E_{ads} (eV)
Phenol on graphite			
AB2 (vi) (vdW-DF)	3.47	0	0.56
AB1 (v) (vdW-DF)	3.47	0	0.55
AB1 (v) (revPBE)	4.77		0.01
AB1 (v) (PW91)	4.19		0.06
Phenol on alumina			
(i) (PW91)	2.00	10.3	0.88
(ii) (PW91)	1.95	44.7	1.00
(iii) (PW91)	1.97	21.3	0.91
(iv) (PW91)	1.98	21.5	0.91

For each of these four initial structures [(i)–(iv) in Fig. 1] the local energy minimum regarding the atomic positions is found by optimizing the atomic positions according to the Hellmann-Feynman forces from the GGA electronic charge density. Upon adsorption each of the initially parallel structures [(i), (iii), and (iv)] are found to tilt its aromatic ring slightly (all phenol atoms are allowed to relax). The final adsorption energies for these structures are found to be very similar and around 0.9 eV. Also the phenol-O to alumina-Al adsorption distances d_{ads} found (1.97–2.00 Å), and the geometrical structures upon adsorption, listed in Table I, are very similar for these three "parallel" structures. As expected, the largest change from the gas phase molecule atomic geometry is associated with the OH group (which binds to the surface), although the changes are small.

A larger GGA binding energy is found for the initially tilted structure (ii). Upon relaxation, the optimum tilt angle found is 44.7°. In this case the angle ∠COH of the adsorbed

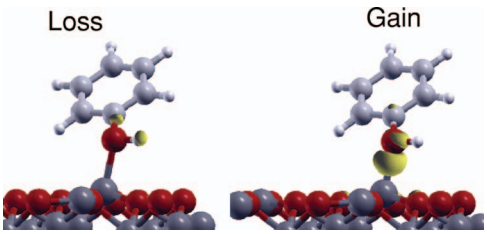

FIG. 2. (Color) Change in electron charge density after adsorption of phenol on α-Al_2O_3(0001) for adsorption structure (ii). The left-hand (right-hand) panel shows the isosurface for loss (gain) of 0.05 $e/Å^3$. Atom color coding as in Fig. 1.

phenol opens up slightly compared to the gas phase molecule, but otherwise the (small) changes are similar to those in the parallel structures. The GGA adsorption energies and separations of the structures (i)–(iv) are given in Table II. The optimal adsorption structure is the "tilted" structure (ii) with adsorption energy 1.00 eV, occurring for $d_{ads}=1.95$ Å, followed in energy by the "parallel" structures. This may be compared with the adsorption energy 1.23 eV for methanol on the same surface.[14] An analysis of the bonding reveals that, similarly to methanol on alumina,[14] the electron density increases in the region of space between the phenol O atom and the alumina Al atom compared to the situation without a bond. However, only the phenol O atom contributes electrons to the bond, see Fig. 2. Methanol and phenol have lone-pair electrons with highest weight on the O atom (cf. H_2O) that interact with the Al atom in the top layer, thus forming a bond of covalent character. The result can be seen in the density plots as an increased electron density between the phenol O atom and the nearest Al atom (Fig. 2).

Although phenol is thus bound to the alumina surface by covalent forces, we have also estimated the contribution to the binding from the vdW interaction. The calculation of the adsorption energy on alumina including the vdW interactions is essentially carried out as for adsorption on graphite. However, a number of issues need to be considered in the alumina study.

First of all, whereas in the graphite adsorption we can rely on the phenol molecule and the graphite surface each remaining geometrically unchanged upon adsorption this is clearly not the case for the adsorption on alumina. Hence, while only one structural parameter (d_{ads}) needs to be energetically optimized in the graphite case a large number of structural parameters, namely the positions of all relevant atoms, must in principle be optimized in the alumina case. This could be carried out in the spirit of Ref. 25, but for the present system it would require an enormous effort. Instead we take advantage of the fact that phenol already in GGA binds rather strongly to alumina and that within GGA the adsorption positions can easily be found by utilizing the Hellmann-Feynman forces (as presented above). The evaluation of the Hellmann-Feynman forces is at present not implemented within vdW-DF. In the present calculations we use this GGA-based structure, making no further structural optimization within vdW-DF, assuming that the GGA-based structure for alumina adsorption is sufficiently close to the real adsorption structure.

Second, the total number of atoms (for the same surface area) is significantly larger for the alumina slab than for the graphene sheet. Upon adsorption the alumina surface relaxes, which makes it difficult to increase the unit cell size for the vdW calculation by simply supplementing with the charge density of a clean surface, as is done here for phenol on graphite, and for benzene and naphthalene on graphite in Ref. 7. Instead, a larger surface area for the vdW-DF calculation must be obtained by using a larger surface cell in the underlying GGA calculation. This is not feasible, given the large number of atoms. Instead we have evaluated the vdW contribution on alumina only for the original (2×2) surface cell (contrary to the case for graphite where the cell is enlarged).

It should be noted that this second issue is not a vdW-DF issue, although also the vdW-DF calculation is affected by it. Rather, the problem is simply that a (2×2) surface unit cell in alumina is slightly too small for the surface atoms furthest from the phenol molecule to be unaffected by the adsorption. Even within GGA the phenol molecule cannot quite be considered an "isolated adsorbant" on the surface.

The evaluation of the vdW contribution on alumina is performed in two steps. In the first step we use vdW-DF to evaluate the energy difference between the adsorption structure and the corresponding "far-apart" system where the atoms have been fixed in their adsorption positions, but where the phenol molecule is translated a large distance (5.8 Å) away from the surface. This is similar to what is done in the graphite case. In the next step we evaluate within standard PW91 the energy gained by relaxing the atom positions in the "far-apart" system to phenol in its gas phase geometry and the alumina surface as a clean surface. This step is redundant in the graphite case because neither the graphene sheet nor the phenol molecule change structure in the adsorption process. The use of the "far-apart" system described above was argued for in Ref. 26 to avoid small spurious energy contributions. In the present system substituting the "far-apart" system directly with systems of isolated phenol and alumina in their respective adsorption geometries yields similar results.

Our vdW-DF calculation of phenol on alumina, similar to the one described for phenol on graphite, indicates a small but not negligible increase in the adsorption energies of the structures studied. The sum of the total energy changes after the vdW correction results in adsorption energies of around 1.1–1.2 eV for all the structures (i)–(iv), making it less clear which is the most favorable structure. While the tendency of structure (i) being the least favorable and (iv) being the next-to-least favorable is preserved, we find that including the vdW contribution makes structure (iii) slightly more favorable than the tilted structure (ii). It is no surprise that the vdW interaction has a larger effect on the nearly parallel structures (i), (iii), and (iv) compared to the tilted structure (ii) because the carbon ring in (ii) is less exposed to the surface as it has the largest adsorption angle of the four, see Table II. Comparing structures (iii) and (iv), which have very similar adsorption angles and distances, we find a larger vdW contribution for (iii). This may be explained by the placement of the aromatic ring in phenol, which for (iii) resembles the more favorable AB stacking.

VI. DISCUSSION AND CONCLUSIONS

Phenol molecules interacting with surfaces constitute interesting prototype systems for such varied phenomena as proteins, polymers (e.g., relation of chain termination to multiscale behavior near surfaces), paint, catalysis, toxicity, and widespread occurrence as a by-product. This calls for an understanding of the interaction, and the possibility of bridging the atomic and macroscopic scales starts to open up. However, understanding of the adsorption step must be established first by careful comparisons between experiment and theory.

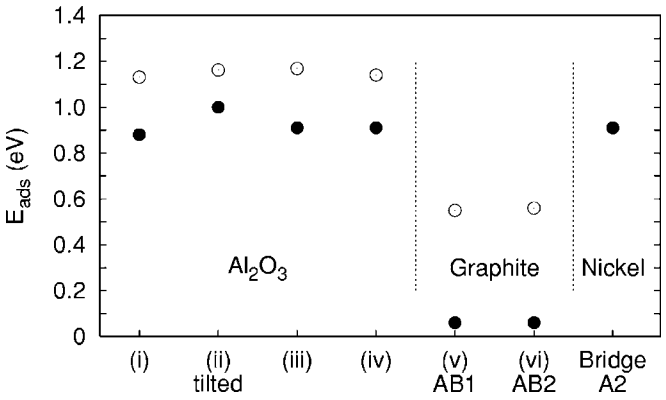

FIG. 3. Adsorption energies of phenol on various surfaces: Alumina (this study), graphite (this study), and Ni(111) (value from Ref. 27). For alumina and graphite the numbers reflect the different adsorption sites and orientations, as named in Fig. 1. For Ni only the energy for the most favorable adsorption site (BridgeA2, with the naming used in Ref. 27) is shown. Solid circles are PW91 calculations [except for Ni where the functional used is the Perdew-Burke-Ernzerhof GGA functional (Ref. 29)] and open circles are calculations using vdW-DF.

While the adsorption of phenol on graphite is clearly of vdW nature, this is not the case for the adsorption on alumina. However, it is of interest to note the relative size of the energetic contribution when including the vdW interactions also in the latter case. It is a significant correction.

As discussed in the preceding section, we use the same method in the two calculations of vdW interactions, but practical limitations force us to treat the vdW-DF in the alumina case somewhat more approximately than the graphite case. Our calculation of the adsorption energy on alumina including the vdW interactions is therefore not quite as rigorous as for phenol on graphite.

Together with the Ni(111) results of Refs. 4 and 27 three types of substrates have been studied, with different bonds to the phenol molecule. On graphite, phenol adsorbs in a clean vdW bond. On α-Al_2O_3(0001), the bond is primarily covalent in nature, that is, similar to the one between methanol and alumina.[13,14] On Ni(111), the bond seems to be metallic, maybe of a donation-backdonation type.[28] No estimate of the vdW interaction between phenol and Ni(111) has yet been provided. The adsorption-energy values for the three surfaces end up in a narrow range, 0.6–1.2 eV (Fig. 3), yet the bonds are characteristically different. As a matter of fact, the covalent bond on alumina and the covalent-metallic bond on Ni are each weak for their classes, whereas on graphite the physisorption bond is a strong one. The differences between these hydrophobic and hydrophilic surfaces are thus illustrated by their different phenol adsorption-energy values and adsorption distances.

The values of the adsorption energies must be compared to other relevant energy values in order to describe the more complex phenomena. To confirm the theoretical adsorption picture, the energy values could be compared with thermal-desorption data, as has been done for, e.g., the PAH's on graphite.[24]

The calculations do not only bring information on energetics but also on geometry. The adsorption distance d_{ads} is similar for all the covalent-metallic bonds (on alumina and on nickel), namely $\sim$2 Å, whereas the pure-vdW bonds (on graphite) yield the larger $d_{ads} \approx 3.5$–4.5 Å. Even if energy differences between different sites and orientations are sometimes small, the calculations give results for atomic positions that should challenge the experimentalists. The scanning-tunneling microscope (STM) here offers outstanding possibilities. STM provides results for adsorbates on several types of substrates, see e.g., Ref. 30. In fact, STM work is presently performed even on several systems that are probably physisorbed or for which at least vdW interactions must be important (e.g., organic molecules with benzene rings). On the latter systems, traditional DFT fails to describe the experimental structure that is seen in the STM. Hopefully the phenol-on-graphene results above (and similar ones coming successively) will stimulate measurements on such systems.

While phenol is physisorbed on graphite, its adsorption is covalent on alumina and metallic (largely covalent) on Ni(111). Also here STM offers great possibilities, as the tunneling-current characteristics should be quite different for the three types of adsorption.

In summary, the results for phenol adsorption on the three types of surfaces, with three types of bonds, are thus very instructive for the understanding of the interaction of organic molecules with surfaces and interfaces relevant in biology.

ACKNOWLEDGMENTS

Partial support from the Swedish Foundation for Strategic Research (SSF) via the ATOMICS consortium, the Swedish Research Council (VR), and NordForsk through a mobility scholarship for one of the authors (Ø.B.) is gratefully acknowledged, as well as allocation of computer time at UNICC (Chalmers) and SNIC (Swedish National Infrastructure for Computing).

[1] S. D. Chakarova and A. E. Carlsson, Phys. Rev. E **69**, 021907 (2004).

[2] M. P. Casaletto, M. Carbone, M. N. Piancastelli, K. Horn, K. Weiss, and R. Zanoni, Surf. Sci. **582**, 42 (2005).

[3] A. C. de Oliveira Pimenta and J. E. Kilduff, J. Colloid Interface Sci. **293**, 278 (2006).

[4] L. Delle Site, C. F. Abrams, A. Alavi, and K. Kremer, Phys. Rev. Lett. **89**, 156103 (2002).

[5] M. Dion, H. Rydberg, E. Schröder, D. C. Langreth, and B. I. Lundqvist, Phys. Rev. Lett. **92**, 246401 (2004); **95**, 109902(E) (2005).

[6] C. Bertocini, H. Odetti, and E. J. Bottani, Langmuir **16**, 7457 (2000).

[7] S. D. Chakarova-Käck, E. Schröder, B. I. Lundqvist, and D. C.

Langreth, Phys. Rev. Lett. **96**, 146107 (2006).
[8] T. Thonhauser, A. Puzder, and D. C. Langreth, J. Chem. Phys. **124**, 164106 (2006).
[9] Open-source plane-wave DFT computer code DACAPO, http://www.fysik.dtu.dk/CAMPOS/
[10] J. P. Perdew, J. A. Chevary, S. H. Vosko, K. A. Jackson, M. R. Pederson, D. J. Singh, and C. Fiolhais, Phys. Rev. B **46**, 6671 (1992); **48**, 4978 (1993).
[11] Y. Zhang and W. Yang, Phys. Rev. Lett. **80**, 890 (1998).
[12] S. D. Chakarova-Käck, J. Kleis, and E. Schröder (unpublished).
[13] Ø. Borck and E. Schröder, ATB Metall. **43**, 342 (2003).
[14] Ø. Borck and E. Schröder, J. Phys.: Condens. Matter **18**, 1 (2006).
[15] H. Rydberg, M. Dion, N. Jacobson, E. Schröder, P. Hyldgaard, S. I. Simak, D. C. Langreth, and B. I. Lundqvist, Phys. Rev. Lett. **91**, 126402 (2003).
[16] H. J. Monkhorst and J. D. Pack, Phys. Rev. B **13**, 5188 (1976).
[17] R. W. G. Wyckoff, *Crystal Structures*, 2nd ed. (Interscience, New York, 1964).
[18] C. G. Broyden, J. Inst. Math. Appl. **6**, 76 (1970); R. Fletcher, Comput. J. **8**, 317 (1970); D. Goldfarb, Math. Comput. **24**, 23 (1970); D. F. Shanno, Math. Comput. **24**, 647 (1970).
[19] NIST Computational Chemistry Comparison and Benchmark Database, NIST Standard Reference Database Number 101, Release 12, Aug 2005, Editor: Russell D. Johnson III, http://srdata.nist.gov/cccbdb
[20] N. W. Larsen, J. Mol. Struct. **51**, 175 (1979).
[21] A. Puzder, M. Dion, and D. C. Langreth, J. Chem. Phys. **124**, 164105 (2006).
[22] H. Rydberg, N. Jacobson, P. Hyldgaard, S. I. Simak, B. I. Lundqvist, and D. C. Langreth, Surf. Sci. **532**, 606 (2003).
[23] D. C. Langreth, M. Dion, H. Rydberg, E. Schröder, P. Hyldgaard, and B. I. Lundqvist, Int. J. Quantum Chem. **101**, 599 (2005).
[24] R. Zacharia, H. Ulbricht, and T. Hertel, Phys. Rev. B **69**, 155406 (2004).
[25] E. Ziambaras and E. Schröder, Phys. Rev. B **68**, 064112 (2003).
[26] S. D. Chakarova and E. Schröder, Mater. Sci. Eng., C **25**, 787 (2005).
[27] L. Delle Site, A. Alavi, and C. F. Abrams, Phys. Rev. B **67**, 193406 (2003).
[28] This interpretation is ours, not from Refs. 4 and 27.
[29] J. P. Perdew, K. Burke, and M. Ernzerhof, Phys. Rev. Lett. **77**, 3865 (1996); **78**, 1396 (1997).
[30] M.-L. Bocquet, H. Lesnard, and N. Lorente, Phys. Rev. Lett. **96**, 096101 (2006).